Model-Based Pupil and Iris Localization

Nitin K. Mahadeo, Andrew P. Papliński, Sid Ray
Clayton School of Information Technology
Monash University
Email: {Nitin.Mahadeo, Andrew.Paplinski, Sid.Ray}@monash.edu

***Abstract*—The iris is the most accurate biometric to date and its localization is a vital step in any iris recognition system. Iris localization can be considered as the search for the demarcation points, or step change in intensity at its boundaries. A failed localization will lead to incorrect iris segmentation and eventually to poor recognition. In the first stage, we proceed with the elimination of reflection and the reduction of lighting variations in eye images. In the second stage of our proposed system, radii and locations of the pupil and iris are obtained by maximizing the convolution of the image with a toroidal 2-D filtering shape derived from the Petrou-Kittler 1-D filter. Such a novel approach delivers robust localization of the inner and outer iris boundaries. We tested our system on a large dataset of poor quality eye images with substantial occlusions, illumination and defocus and the proposed algorithm is found to be robust and accurate.**

***Index Terms*—Biometrics, Iris localization, 2-D filters, Petrou-Kittler filter**

I. Introduction

Iris recognition has received much attention for the past few years and a lot of research is actively being carried out in this area. The iris is the most accurate biometric to date and outperforms its many counterparts. Its rich texture being quite stable for a long period of time makes it suitable for identification and recognition purposes. In addition, no physical contact is required as opposed to other biometrics such as fingerprints. On the other hand, capturing a good eye image can be challenging since it is a relatively small moving target on a wet and reflective surface. So far, most iris recognition systems developed have been carried out on eye images captured in controlled environments and iris localization has been relatively straightforward. Impressive results have been reported using these types of images. However, eye images captured in uncontrolled environments often contain reflections and illumination variations. They are also often deformed, out of focus and off-angle. This is still an open problem. For iris recognition to be widely adopted, it needs to be segmented in an accurate and reliable way in non-cooperative environments. This makes the iris localization stage even more critical.

The most significant contributions in the area of iris recognition are those of Daugman [1] and Wildes [2]. Daugman's technique has been commercialized and implemented in several iris recognition systems. It is basically a circular edge detector which searches for the maximum of the contour integral derivative in the blurred image. On the other hand, Wildes' technique searches for an ellipse in the edge image using Hough transform to segment the iris. Recently, some researchers have begun to focus their research on the segmentation of non-ideal eye images i.e., images captured in challenging environments, for example images with poor contrast between the iris boundaries, specular reflections, eyelashes, etc.

Here, we briefly mention some of the recent work that has been carried out to tackle the localization problem in iris images. In [3], a push and pulling method is implemented to locate the iris but an initial estimate of the pupil's centre is required for accurate and fast localization. In [4], geodesic active contour is used for iris segmentation but the stopping criterion does not take into consideration the amount of edge information and might miss the iris boundaries. Moreover, this approach will fail if the contour is not initialized close to the iris boundaries.

Being able to correctly identify and recover iris boundaries in occluded and poor quality eye images is the main objective of our work. In this paper, we present a novel model-based algorithm for fast and accurate iris localization. In our method, the pupil and iris radii and locations are obtained by maximizing the convolution of the image with a toroidal 2-D filtering shape derived from the Petrou-Kittler 1-D filter [5]. Such a novel approach delivers robust localization of the inner and outer iris boundaries. In our experiments, no prior assumptions are made on the position of the pupil or the iris in the image, the amount of occlusion or the type of illumination being used as opposed to images captured in [1].

The rest of the paper is organized as follows: in Section II we discuss the pre-processing of the close-up eye images and in Section III, the implementation of our iris localization model. In Section IV, we present our results and analysis. Finally, in Section V, we present our conclusions and suggestions for future work.

II. Preprocessing

Artifacts such as defocus, reflections and lighting variations are present in the real-life images images of the eye. Elimination of those artifacts facilitates the localization of iris borders. In this Section, we describe the process of eliminating reflections followed by the implementation of an illumination invariance based technique for image quality improvement as discussed below.

A. Specular reflections

Specular reflections are sharp bright dots which often appear on the Region of Interest (ROI) in the eye image i.e., on the

pupil, pupil-limbus border and limbus. These reflections can mislead the algorithm into considering these step changes in intensity level as boundaries. This can, in turn, degrade performance and needs to be taken into consideration. Reflections can easily be identified since they lie close to the maximum intensity values. Let $I(x, y)$ be the intensity value at location (x, y) in image I, then using a simple thresholding technique, given by $I(x, y) > T$, where T is the threshold, these pixels can be identified. It is important to point out that the optimum threshold for detecting those pixels responsible for reflection will vary depending on the environment and cameras used to capture the images.

Once localized, a morphological operation, namely dilation, is used to find the intensity values and locations of reflections and that of its neighbouring pixels in the image. The neighbouring pixels are used to compensate for the missing areas i.e., they contribute a small fraction of their intensity and smoothly propagate the information to the missing areas. In our experiments, this in-painting algorithm is implemented using a sparse based partial differential equation similar to that in [6], [7]. As shown in column 2 of Fig. 1, the effect of reflections in the eye images from column 1 of Fig. 1 has been significantly reduced. This is particularly noticeable in the pupillary area where the algorithm has filled in those regions containing reflections with information surrounding them. Other regions successfully detected as containing reflections and in-painted include the tear ducts. The advantage of this localized approach is that only affected regions are taken into consideration and information in other regions remain untouched as opposed to applying a median filter over the whole image [8].

B. Illumination

Illumination due to light sources at arbitrary positions and intensities are responsible for a significant amount of variability in an image. It can drastically change the appearance of the image and these lighting variations affect the accuracy of iris recognition. To solve this problem, we implemented the Retinex algorithm to handle the lighting effect. This technique was originally proposed by Land and McCann in [9] and aims to bridge the gap between captured images and the human visual system and has been successfully applied in several areas such as medical radiography, underwater photography, and face recognition systems. The basic idea of the Retinex algorithm is as follows: by breaking down an image $I(x, y)$ into its luminance and reflectance components as in (1):

$$I(x, y) = R(x, y) \times L(x, y) \tag{1}$$

it is possible to remove the effect of illumination and enhance images with lighting variations. The Single Scale Retinex (SSR) is given by:

$$R(x, y) = \log I(x, y) - \log[F(x, y) \circ I(x, y)] \tag{2}$$

where $I(x, y)$ is the input image, '$\circ$' represents a convolution operation, $R(x, y)$ is the output image and $F(x, y)$ is the surround function which can be mathematically represented by:

$$F(x, y) = Ke^{-\frac{x^2+y^2}{c^2}} \tag{3}$$

where K and c are constants. One disadvantage of the SSR is that it is limited by the range of the scale, i.e., it can only achieve tonal rendition or dynamic range compression at the expense of each other. The Multi-Scale Retinex (MSR) algorithm is an extension of the SSR and overcomes this limitation of the SSR. It is basically the multi-scale form, i.e., the weighted sum of SSRs is shown in (4):

$$R(x, y) = \sum_{k=1}^{N} w_k \left\{\log I(x, y) - \log\left[F(x, y) \circ I(x, y)\right]\right\} \tag{4}$$

In this work, we implemented the MSR algorithm after the reflection elimination stage described in the previous sub-section. The MSR algorithm can achieve both dynamic range compression and tonal/lightness rendition and hence is particularly suited for eye images captured in different lighting conditions [10]. Column 3 of Fig. 1 illustrates the effect of the Retinex algorithm on sample eye images. In Fig. 1(c), the contrast between the pupil and the iris is much higher and in Fig. 1(f), the dark areas in the image are enhanced and more details are visible. Overall, the preprocessing step significantly improves the image quality thereby facilitating inner iris border localization in eye images.

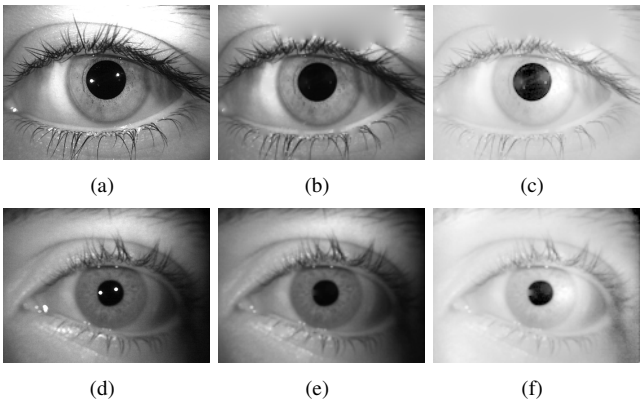

Fig. 1: Preprocessing of an eye image: (a) and (d) are the original eye images, (b) and (e) show the result of in-painting on the original images in column 1, (c) and (f) show the effect of Multi-Scale Retinex applied to the in-painted eye images in column 2

III. The localization model

In this section, we briefly describe the limitations and specifics of some of the common iris localization techniques followed by a detailed description of our algorithm, its implementation and how it overcomes the shortcomings of previous methods. The majority of iris segmentation techniques use hard thresholding to locate the pupil in eye images. Edge detection techniques such as Canny and Sobel are then used to

obtain an edge image to search for the outer iris boundary as in [6], [11]. These edge detection methods are also threshold dependent and need to be adjusted depending on the quality of the image. Therefore, they often lead to incorrect detection of iris borders in images with thick eyelashes, strong specular reflections and poor contrast between the pupil and the iris. In addition, circular Hough transform, a computationally intensive technique is often used to fit a circle or an ellipse to the binary edge image. In [8], around 30 control points are drawn perpendicular to the circumference of an ellipse. The intensity profile at each control point is then convolved with two Petrou-Kittler 1-D ramp filters [5] of different width, and the maxima for different radii are computed using simulated annealing (SA) as an optimization technique.

A. The proposed 2-D toroidal filter

Similarly to [8], we have also based our model on the 1-D Petrou-Kittler filter since it is particularly well-suited for ramp edges prevalent in our eye images characterized by a gradual change in intensity. According to the Petrou-Kittler model, the positive half of the 1-D edge filter can be represented by following expression:

$$\begin{aligned} s(r) \quad = \quad & 1 + be^{-r} - r_1 e^{ar}\cos(ar+\alpha_1) \\ & + r_2 e^{-ar}\cos(ar+\alpha_2), \quad \text{for} \quad 0 \le r \le w, \\ & \text{and} \quad 0 \quad \text{otherwise} \end{aligned} \tag{5}$$

where w is the span of the half-filter. More information on the practical implementation of the 1-D Petrou-Kittler filter and its parameters a, b, r_1, r_2, α_1, and α_2 used in expression (5) can be found in [5], [12]. As an illustration, the 1-D edge half-filter of width $w = 4$ is shown in Fig. 2.

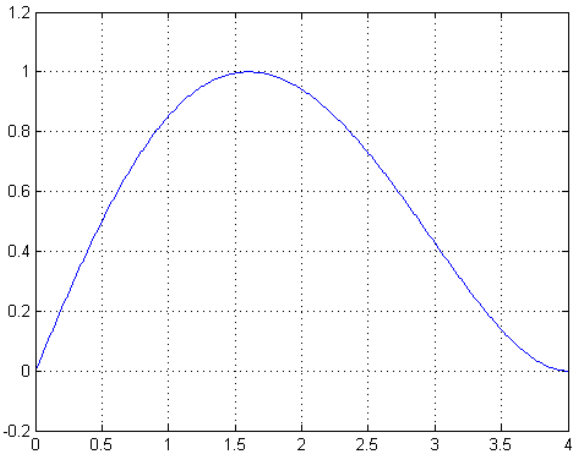

Fig. 2: 1-D Petrou-Kittler edge half-filter of span $w = 4$

The next step deals with the extension of the 1-D Petrou-Kittler edge filter to a 2-D toroidal filtering shape for iris localization. The main idea behind our model is to find the best location (x_c, y_c) of a circle of a radius R that localizes the pupil and the iris in an eye image. Such a circle should go through the edges of the pupil or iris. To create a 2-D filter that can localize the circle, we place a 1-D filter specified in (5) at a distance R from the centre and rotate it to form a 2-D toroidal filtering shape as shown in Fig. 3. Formally, the filtering surface can be described in polar coordinates (r, θ) in the following way:

$$h(r,\theta;R,w) = \begin{cases} s(r-R) & \text{for} \quad R \le r \le R+w \\ -s(R-r) & \text{for} \quad R \le r-w \le R \\ 0 & \text{otherwise} \end{cases} \tag{6}$$

where R is the expected radius of the iris or pupil and w is the width of the underlying 1-D filter. The square section of the function $h(r, \theta; R, w)$ of size $2(R + w) \times 2(R + w)$ is then converted into a square matrix $H(x, y)$ of an equivalent dimension for given values of the parameters R and w. A colour coded implementation of our 2-D filter $H(x, y)$ from Fig. 3 is shown in Fig. 4.

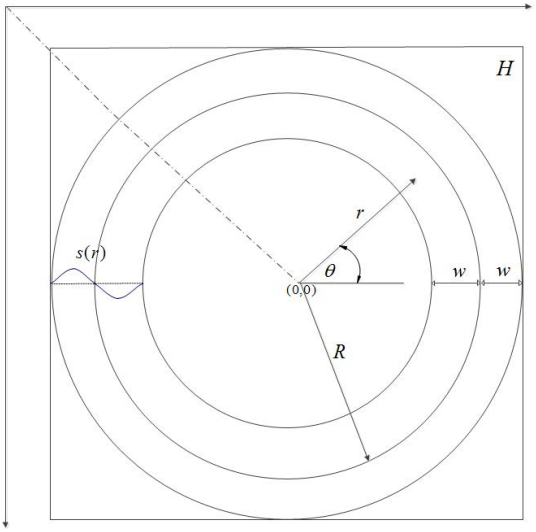

Fig. 3: 2-D toroidal shape based on the Petrou-Kittler 1-D filter where $s(r), w$ and R are described in expressions (5) and (6)

B. The proposed localization method

After the 2-D filter $H(x, y)$ has been created for a given radius R, the next step is to calculate the convolution of the image $I(x, y)$ with the filter as in the following expression:

$$Q(x,y) = I(x,y) \circ H(x,y) \tag{7}$$

where $\circ$ is the convolution operator. The convolution $Q(x, y)$ can be thought of as a performance function to be maximised. The maximum of the convolution matrix entry gives the centre of the circle, (x_c, y_c) of the radius R that optimally fits a potential iris or pupil. The process is iterated over a required range of the radii R. Practical implementation of the convolution can be performed by an equivalent linear neural network operation.

The transition at the pupillary and outer iris boundary is modelled using Petrou-Kittler 1-D filter at different scales.

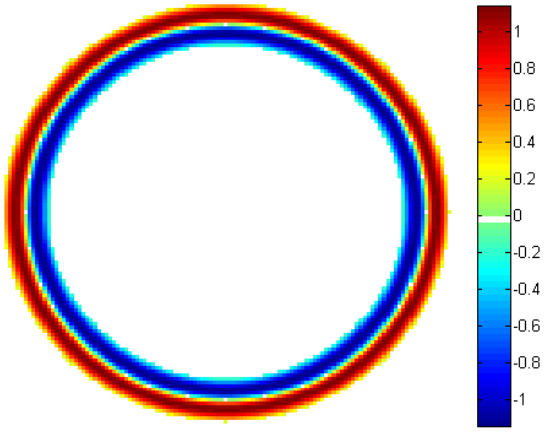

Fig. 4: Colour-coded 2-D toroidal model derived from 1-D Petrou-Kittler edge filter

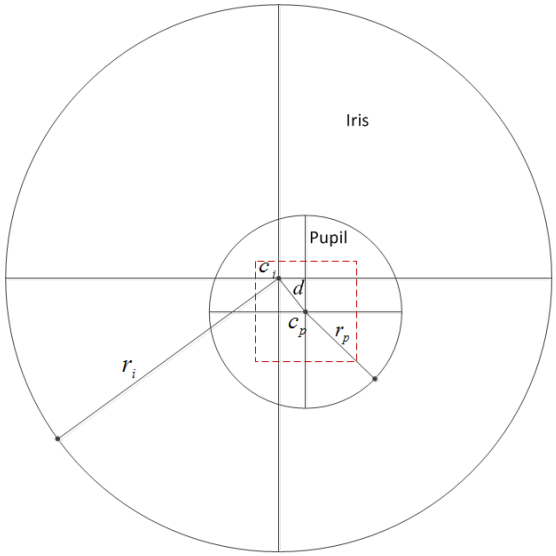

Fig. 5: Spatial location of the pupil and iris parameters where c_p and c_i are the centres of the pupil and the iris, r_p and r_i are the radii of the pupil and the iris and d is the distance between them

A filter of smaller width, w, is used to model the inner iris boundary (the pupil) since the contrast from pupil to iris is higher compared to the transition at the outer iris border which can be extremely smooth, hence, a wider filter with a higher value of w is employed.

In our experiments, an initial search of the pupil as a result of its higher contrast followed by localization of the outer limbus proved to be very effective. When searching for the outer iris border, the following considerations are taken into account. Firstly, the transition between the iris and the sclera is very smooth. Secondly, the iris region is often occluded by eyelids and eyelashes. It contains reflections and lighting variations which can severely impact quality of the image.

In general, the pupil and the iris do not share the same centres, as indicated in Fig. 5. They are relatively close to each other, taking into consideration factors such as pupillary dilation and constriction in different environments. In Fig. 5, $c_p = (x_{cp}, y_{cp})$ and $c_i = (x_{ci}, y_{ci})$ are the centre coordinates of the pupil and the iris respectively. Similarly, r_p and r_i are the radii of the pupil and the iris and d is the displacement between c_p and c_i.

Once the pupil is localized, instead of searching the entire image $I(x, y)$ again for the outer iris boundary, we restrict our search for the centre coordinates of the iris based on the following heuristics. Extensive testing was carried out on a subset of the dataset and the average distance between the pupil and iris centres, d_{avg}, was found to be 3 pixels and the maximum value, d_{max}, 6 pixels. d_{max} usually occurs in images with severe dilation or strong illumination. It follows that the optimum spatial location of potential iris centres can thus be defined an area with radius d_{max} from the pupil's centre, c_p. This is shown by the dotted line in Fig. 5 and this region indicates the the maximum likelihood of finding an accurate iris centre, c_i. We need to keep in mind that the d_{max} and d_{avg} will change based on the resolution of the images captured by the iris sensors.

This approach has two main advantages. In addition to improving the speed of the process by avoiding the need for a second exhaustive search to find the parameters of the outer iris boundary, the accuracy and robustness of the localization process is also preserved.

Finally, we would like to highlight some of the differences of our model with other implementations which may bear some resemblance at the top level. In [8], at each control point, the summation over the length of the 1-D Petrou-Kittler filter of the product of the intensity profile and that of the filter mask is computed and accumulated. The energy functional is subsequently minimized using simulated annealing (SA) to find the optimum parameters of the iris. Filtering only at control points can lead to incorrect localization, important edges can be missed. Furthermore, this model requires an implementation of a complex, time-consuming optimization technique to find the minimum of the cost function in the image. This is replaced, in our case, by finding a maximum in the convolution matrix. Daugman presents in [1] another model-based technique. Although from a very brief description it is difficult to compare the two methods precisely, the central to the explanation of the Daugman's method is the following equation that we adopted from [1]:

$$\max_{(r,x_0,y_0)} \left| G_\sigma \circ \frac{\partial}{\partial r} \oint_{r,x_0,y_0} \frac{I(x,y)}{2\pi r} ds \right| \tag{8}$$

Equation (8) suggests that his technique implies three operations: a circular filter, calculation of the gradient, and low-pass filtering. In our case, not only the order of the operations is reversed, the low-pass filtering being the first operation as suggested by a very successful Canny filter [13], but also the

three operations are carried out in one convolution operation with our 2-D toroidal filter.

IV. Experimental results

In this section, we present our results and discuss the performance of our algorithm in terms of its localization accuracy and running time. We compare and discuss our findings followed by the contributions of our iris localization model.

A. Performance

The WVU Multi-modal Biometric Dataset was used to evaluate the performance of our algorithm [14]. In all, 3806 images were used. WVU Release 1 contains 3043 images of 231 subjects and WVU Release 2 contains 763 images of 72 subjects. The images were captured using an OKI IRISPASS-h hand-held device and have a resolution of 640×480 pixels. This dataset has been confirmed to contain non-ideal images that are significantly inferior compared to other available datasets, i.e., they were captured without any quality control [15]. We compare our localization method with three well known methods, namely those of Zuo and Schmid [6], Masek [16] and Wildes [2].

A correct segmentation is one where there is no distinct offset between the boundary of the iris and that of the circle. For consistency, the same metric used by Zuo and Schmid in [6] is used in this paper to identify correct localization and evaluate the performance of our segmentation algorithm. The amount of occlusion is not considered in our experiments. Experimental results are tabulated in Table I, from which we

TABLE I: Performance of Iris Localization Techniques [6]

Dataset	Masek [16]	Wildes [2]	Zuo & Schmid [6]	Proposed
WVU	64.8	85.2	97.9	94.3

can see that our localization success rate is significantly higher than those of Wildes or Masek and comparable to that of Zuo and Schmid. It is also noteworthy in this respect to mention that the results reported by Zuo and Schmid in [6] were carried out on only 2453 images from the WVU dataset while in this paper, the success rate being reported includes 3806 images, i.e., all images from both Release 1 and Release 2 of WVU dataset are used in our experiments.

Fig. 6 shows some examples of iris localization using our 2-D toroidal filter and its performance on images from the WVU Dataset. The first row shows the localization result in images with reflections close to or on the pupillary border. In the second row examples of recovered pupil and iris boundaries in images with substantial lighting variations and poor contrast between the pupillary area and iris region are shown and finally, the third row demonstrates the performance of our proposed methodology on images with eyelashes and various levels of occlusion. It is interesting to note that our algorithm which approximates the inner and outer boundaries of an iris works well even in really difficult cases.

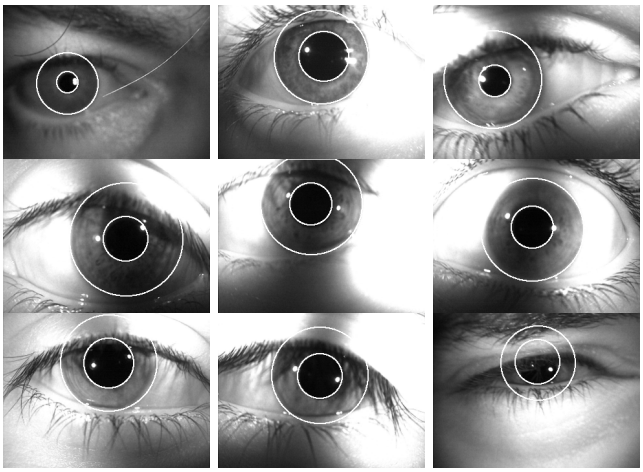

Fig. 6: Examples of pupil and iris localization in images with substantial occlusions, reflections and illumination variations

Fig.7 shows some examples where our algorithm failed to detect the iris boundaries. Overall, the types of error we encountered in the WVU dataset can be grouped in 3 broad categories. The first type of error can be referred to as the near-optimal category, i.e., images in which the iris boundary detected by the model-based filter is close to the actual iris boundary but does not fall exactly on it. This occurs when there are shadows, blur or poor contrast near the iris boundary. Occlusion or non-circular shape of the iris also account for this type of failed localization. This type of error was most common, 152 such incorrect localizations were identified in the WVU dataset. Two examples of incorrect iris detection which fall in the first category are shown in Fig. 7(a) and Fig. 7(b).

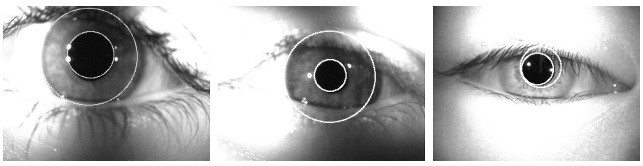

(a) (b) (c)

Fig. 7: Examples of eye images on which the proposed algorithm failed to perform: (a) and (b) are examples of images where the boundary detected is close to the actual iris boundary but does not fall exactly on it and (c) is an example where the pupil was successfully localized but the iris was incorrectly detected.

The second category consists of eye images in which the pupil was successfully localized but the iris was incorrectly detected. We refer to this type of errors as poor localization. In this case, the cost function incorrectly detected the outer iris boundary. There were 58 eye images in this category. An example of this type of incorrect localization is shown in the Fig. 7(c).

Finally, the third type of error was found in images in

which localization failed completely, i.e., images captured by the sensors were of very poor quality and both pupil and iris localization failed. There were only 6 images in this category.

Before concluding this section, we would also like to add that our 2-D toroidal filter performed unexpectedly well in some images with a significant degree of difficulty such as blur, occlusion or poor distinction between the inner and outer iris boundaries. Some examples of such localizations are shown in Fig. 8.

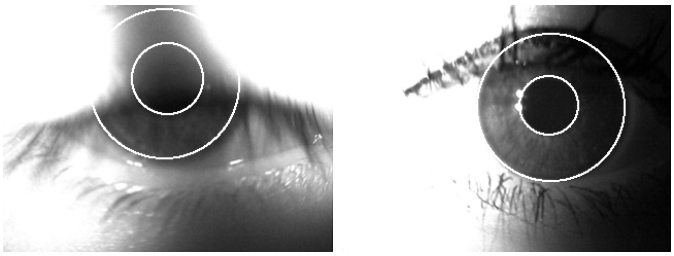

(a) (b)

Fig. 8: Examples of iris localization using the proposed technique on some difficult images in the WVU dataset

B. Computation time

In this section we compare the running time of our algorithm with that of other iris localization techniques bearing in mind that image resolution, computing power and datasets used will vary from one implementation to another. Table II shows the speed of some well known techniques implemented in MATLAB [17] and C++ [6], [18].

TABLE II: Comparison of Image Resolution, Algorithm, Platform and Running Time [6], [18]

Resolution	Algorithm	Platform	Time [s]
400 × 300	Proença and Alexandre	C++	2.3
400 × 300	Daugman	C++	2.7
400 × 300	Wildes	C++	2.0
350 × 270	Trucco and Razeto	Matlab	5.0
320 × 240	Zuo and Schmid	Matlab	30.0
320 × 240	Proposed	Matlab	2.6

The time reported in Table II is the mean time of the localization process on 100 distinct images. In the proposed localization method, the search for the maximum of the convolution operation for different radii is independent of each other. This makes it possible to make efficient use of Matlab optimization techniques and achieve noteworthy speed. Also, considering the fact that variations in image resolution are small, the proposed 2-D toroidal model achieves far superior speed compared to other MATLAB implementations. Moreover, the execution speed of our MATLAB technique is even comparable to C++ based implementations.

C. Analysis

Finally, in this section we discuss the contributions of this paper. The in-painting and MSR algorithm are particularly effective in enhancing the image quality and reducing the effect of illumination in our images. This eases localization of the pupillary boundary. The key contribution in this paper is the extension of the 1-D Petrou-Kittler filter to a 2-D toroidal filtering shape, which achieves high localization rate and robustness in close-up degraded images. As opposed to popular iris localization techniques such as those developed by Wildes [2] or Masek [11], [16], our technique is not threshold dependent. There is only **one** adjustable parameter, namely the width of an underlying 1-D filter. We use $w = 3$ for the sharper inner iris edges, and $w = 6$ for the softer outer ones. We also avoid the need of computationally intensive circle fitting techniques such as Hough transform to fit a circle to the edge image to recover the iris shape or optimization techniques such as SA which can be time consuming.

We would like to have our comment regarding whether the model that we use to approximate the iris boundaries should be a circular or an elliptical one. In our experiments, a circular model was found to be adequate for the purpose of accurately localizing the inner and outer iris boundaries in eye images. The elliptic model just adds two more parameters to the picture without an obvious benefit, but slowing the algorithm down. Moreover, it needs to be emphasized that the shape of filter can be easily extended to an ellipsoidal based shape if required, rotating the 1-D filter along an ellipse rather than a circle. That will be an interesting extension if required.

Another interesting point is that although localization was successful as shown in Fig. 6, the quality of the iris also needs to be taken into consideration prior to the encoding stage especially when it comes to images captured in uncontrolled environments. Finally, the performance of Daugman's method is proportional to the quality of eye images and small intensity change between the iris and the sclera and eyelid occlusion lead to incorrect segmentation [3], [15]. The same trend is observed in Wildes technique, i.e., a significant deterioration in localization with noisy images is observed [18]. With the implementation of a 2-D toroidal filter based on the 1-D Petrou-Kittler ramp filter, we overcome those limitations and our proposed technique achieves high localization rate in images which suffer poor contrast, strong variations in illumination and occlusion.

V. Conclusions

In this paper, a new iris localization methodology for robust iris localization designed specifically for non-ideal eye images is proposed. In the first stage, the effect of specular reflections and illumination variations in eye images is reduced using in-painting and the Retinex algorithm respectively. This is followed by the application of a 2-D toroidal filter based on the 1-D Petrou-Kittler edge filter for pupil and iris localization. Our model is further fine tuned by taking into account the properties and characteristics of the pupil and the iris and how they are related to each other. High performance is achieved on a large dataset non-ideal images from WVU. In our future work, we will focus on off-angle eye images and eye image quality assessment.

ACKNOWLEDGEMENT

The authors would like to thank West Virginia University for granting access to their dataset of eye images.

REFERENCES

[1] J. Daugman, "How iris recognition works," *IEEE Transactions on Circuits and Systems for Video Technology*, vol. 14, pp. 21–30, 2002.

[2] R. Wildes, "Iris recognition: an emerging biometric technology," *Proceedings of the IEEE*, vol. 85, no. 9, pp. 1348–1363, September 1997.

[3] Z. He, T. Tan, and Z. Sun, "Iris localization via pulling and pushing," in *Pattern Recognition, 2006. ICPR 2006. 18th International Conference on*, vol. 4, 0-0 2006, pp. 366–369.

[4] S. Shah and A. Ross, "Iris segmentation using geodesic active contours," *Information Forensics and Security, IEEE Transactions on*, vol. 4, no. 4, pp. 824 –836, December. 2009.

[5] M. Petrou and J. Kittler, "Optimal edge detectors for ramp edges," *IEEE Transactions on Pattern Analysis and Machine Intelligence*, vol. 13, pp. 483–491, 1991.

[6] J. Zuo and N. Schmid, "On a methodology for robust segmentation of nonideal iris images," *Systems, Man, and Cybernetics, Part B: Cybernetics, IEEE Transactions on*, vol. 40, no. 3, pp. 703–718, June 2010.

[7] M. Bertalmio, G. Sapiro, V. Caselles, and C. Ballester, "Image inpainting," in *Proceedings of the 27th annual conference on Computer graphics and interactive techniques*, ser. SIGGRAPH '00. New York, NY, USA: ACM Press/Addison-Wesley Publishing Co., 2000, pp. 417–424.

[8] E. Trucco and M. Razeto, "Robust iris location in close-up images of the eye," *Pattern Anal. Appl.*, vol. 8, pp. 247–255, November 2005.

[9] E. H. Land, John, and J. Mccann, "Lightness and retinex theory," *Journal of the Optical Society of America*, pp. 1–11, 1971.

[10] V. Struc, J. Zibert, and N. Pavesic, "Histogram remapping as a preprocessing step for robust face recognition," *WSEAS Trans. Info. Sci. and App.*, vol. 6, pp. 520–529, March 2009.

[11] K. W. Bowyer, K. Hollingsworth, and P. J. Flynn, "Image understanding for iris biometrics: A survey," *Comput. Vis. Image Underst.*, vol. 110, pp. 281–307, May 2008.

[12] A. Paplinski, "Directional filtering in edge detection," *Image Processing, IEEE Transactions on*, vol. 7, no. 4, pp. 611–615, April 1998.

[13] J. Canny, "A computational approach to edge detection," *Pattern Analysis and Machine Intelligence, IEEE Transactions on*, vol. PAMI-8, no. 6, pp. 679–698, November 1986.

[14] S. Crihalmeanu, A. Ross, S. Schuckers, and L. Hornak, "A protocol for multibiometric data acquisition, storage and dissemination," WVU, Tech. Rep., 2007.

[15] N. D. Kalka, J. Zuo, N. A. Schmid, and B. Cukic, "Image quality assessment for iris biometric," *Biometric Technology for Human Identification III*, vol. 6202, no. 1, p. 62020D, 2006.

[16] L. Masek, "Recognition of human iris patterns for biometric identification," Master's thesis, University of Western Australia, 2003.

[17] "Matlab," Natick, Massachusetts, US.

[18] H. Proenca and L. Alexandre, "Iris segmentation methodology for noncooperative recognition," *Vision, Image and Signal Processing, IEE Proceedings* -, vol. 153, no. 2, pp. 199–205, April 2006.